Technical Physics, Vol. 46, No. 6, 2001, pp. 743–748. Translated from Zhurnal Tekhnicheskoĭ Fiziki, Vol. 71, No. 6, 2001, pp. 104–109.

Solid-Phase Reactions and the Order–Disorder Phase Transition in Thin Films

V. G. Myagkov, L. E. Bykova, G. N. Bondarenko, G. V. Bondarenko, and F. V. Myagkov

Kirenskiĭ Institute of Physics, Russian Academy of Sciences, Siberian Branch, Krasnoyarsk, 660036 Russia

e-mail: kim@ksc.krasn.ru

Received August 29, 2000

Abstract—A comparative analysis was carried out of the initiation temperatures of solid-phase reactions in bilayer solid films and the Kurnakov temperatures of the phases forming in the reaction products. It has been shown that in superstructures where ordering is usually observed, the Kurnakov temperature coincides with the initiation temperature of the solid-phase reactions if no other solid-phase structural transformation precedes the order–disorder phase transition in the state diagram. A rule was proposed by which pairs of films capable of entering into solid-phase reactions and their initiation temperatures can be determined. © *2001 MAIK "Nauka/Interperiodica".*

INTRODUCTION

Solid-phase reactions in thin films, the backbone of modern microelectronics technology, have been intensively studied for the past three decades [1–8]. The majority of the solid-phase reactions in thin metal films occur in the temperature range 400–800 K and fall into two classes. The first class are reactions in which new phases are formed. The second class are reactions whose products contain no new phases while the layers intermix at temperatures below the eutectic temperature [1]. It is believed that the basic mechanism of the low-temperature solid-phase reactions in thin films is the diffusion along grain boundaries, which is several orders of magnitude faster than diffusion in bulk samples [1]. The grain boundary diffusion and high imperfection of the films are the main factors in the formation of compounds at the interfaces of film condensates. As in bulk samples, the formation of new phases in films occurs by nucleation and growth obeying the kinetic Kolmogorov–Avrami–Johnson–Mehl law. Such an analysis supposes that, by virtue of the Arrhenius dependence of diffusion on temperature, the formation of new phases at the interface occurs at any temperature and the thickness of the layer of reaction products depends only on temperature and the annealing time. However, calorimetric data and Rutherford backscattering investigations of many solid-phase reactions in thin films show that the phase formation begins at a certain temperature and proceeds at a fast rate in a narrow temperature interval [2, 3]. Generally, as the temperature is increased, a so-called first phase forms at the interface. Further increase of the temperature can result in the emergence of new phases and the formation of a phase sequence [2–8]. Different rules have been proposed to predict the first phase and the phase sequence [6–8]; however, not one of them can embrace the diversity of experimental data. Nevertheless, prediction of the pairs between which the solid-phase reactions are possible, of the initiation temperature values, of the first phases, and of the phase sequences is extremely important for technical applications.

One of the thermal treatment methods causing solid-phase reactions in thin films to yield compounds is rapid thermal annealing [9]. Rapid thermal annealing includes rapid heating of the sample to a certain temperature, exposure for 1–100 s, and subsequent rapid cooling. It has been shown [10, 11] that solid-phase reactions in metallic thin films can proceed as a self-propagating high-temperature synthesis (SHS). Unlike SHS in powders [10,11], SHS in thin films can occur spontaneously only when the sample temperature T_s exceeds the initiation temperature T_0 ($T_s > T_0$) and represents a surface combustion wave. The SHS front velocity increases exponentially with the sample temperature T_s, and at a sample temperature close to the initiation temperature it is equal to $\sim 2–10 \times 10^{-2}$ m/s. So, the time of travel of the SHS wave over the sample surface in the experiments is equal to ~5–15 s. This suggests that many of the solid-phase reactions taking place in the course of the rapid temperature annealing are SHS reactions. SHS in thin films, the same as the solid-phase reactions, can be of two types. The reaction products formed in the wake of an SHS wave of type I contain compounds. SHS of type II comprises a combustion wave and a phase immiscibility wave, which arises when the sample temperature T_s drops below the initiation temperature T_0. Reaction products of type II SHS in bilayer film systems described by a simple eutectic state diagram contain initial components. Therefore, in such samples, the reaction produces the effect of intermixing of the layers. SHS of type II, called multiple SHS [12, 13], corresponds to the transi-

1063-7842/01/4606-0743$21.00 © 2001 MAIK "Nauka/Interperiodica"

tion through the eutectic temperature in bulk samples. Unlike the eutectic crystallization of the bulk samples, the multiple SHS in thin films is a reversible solid-state structural phase transition. This result is absolutely unexpected since the phase immiscibility observed during eutectic crystallization is currently believed to be the result of the transition of the liquid eutectic into a solid one. Therefore, the multiple SHS should be considered as a "solid-phase melting" of eutectic systems.

The SHS initiation temperatures in many of the bilayer film samples are found in the temperature range 400–800 K, characteristic for solid-state reactions. Comparison with the binary phase equilibrium diagrams of the bulk samples shows that in the temperature range 400–800 K, many structural solid-phase transformations take place. This is an indication that the temperatures of the solid-phase reactions (including SHS) coincide with the phase transformation temperatures. However, it is considered that all these transformations depend on diffusion (excluding the martensite transitions), which is slow in this temperature range and cannot create the considerable mass transfer across the interface between the layers characteristic for SHS and solid-state reactions. Nevertheless, the supposition that the SHS initiation temperatures in thin films are the same as the temperatures of other solid-phase transformations was verified for bilayer systems S/Fe and Cu/Au. In [14], the SHS initiation temperature in S/Fe thin films has been shown to be in agreement with the temperature of the metal-dielectric phase transition in ferric monosulfide FeS. It was shown in [15] that the Kurnakov temperature of the order–disorder phase transition in the classic Cu–Au system determines the initiation temperature of SHS in the Cu/Au bilayer film system.

The present study aims to provide an experimental proof that, in other bilayer film systems as well, the initiation temperature of the solid-phase reactions is determined by the Kurnakov temperature of the ordering phases forming in the reaction products.

SAMPLES AND EXPERIMENTAL TECHNIQUE

The objects studied were bilayer film samples, which could contain ordered phases in the reaction products after passage of an SHS wave or a solid-phase reaction. The systems chosen for comparing Kurnakov temperatures and the initiation temperatures of solid-phase reactions were those in which the ordering phenomenon typically occurs, namely, Cu–Zn, Ni–Zn, Mn–Ni, Co–Al, Fe–Al, Ni–Al, Cu–Al, Ti–Al, Co–Pt, Au–Cu [16–18]. Bilayer film samples were prepared by consecutive vacuum deposition of the above metals onto glass and mica substrates as well as onto freshly cleaved MgO(001) surfaces. The thickness of the layers was chosen such that the composition of the samples after the reactions have been completed was in the region of homogeneity of the ordering alloys studied. The total thickness of the film sample did not exceed 250 nm. In order to improve adhesion and obtain monocrystalline layers on the MgO(001) surface, on all substrates the first layers were deposited with the substrate temperature kept at 500–520 K. To prevent the reaction from occurring during deposition, the second layer was deposited at room temperature. The samples obtained were placed on a tungsten heater in vacuum and heated to the SHS initiation temperature at a rate of no less than 20 K/s. After passage of the SHS front, which was monitored visually, the samples were cooled down at ~10 K/s. In the cases where passage of the SHS front was discernible poorly or not at all, the samples were subjected to rapid thermal annealing. The rapid thermal annealing (RTA) included heating of the bilayer samples at a rate of no less than 20 K/s to a temperature 20–40 K above T_0 and exposition at that temperature for 15 s (the time necessary for passage of the SHS front) with subsequent cooling at a rate of ~10 K/s. Sample preparation and thermal annealing were carried out in a vacuum of $\sim 1 \times 10^{-5}$ torr. The initiation temperature depended strongly not only on the heating rate but also on the thickness of the substrate. Therefore, in the experiments, the substrate thickness was kept at a minimum. For the glass and mica substrates, it was 0.10–0.18 mm; for the MgO substrates, 0.35–0.40 mm. The phase composition was determined using a DRON-4-07 (LOMO) instrument and K_α radiation. The X-ray spectral fluorescence method was used for determining the chemical composition and thickness of the layers. Measurements of the magnetic crystallographic anisotropy were carried out by the method of rotation moments. The degree of transformation η was determined from variation of the magnetic moment of the ferromagnetic sample layer before and after the reaction following the method described in [10, 11].

EXPERIMENTAL RESULTS AND DISCUSSION

Cu–Zn system. In the Cu–Zn system, a β'-CuZn phase of type B2 ordering exists. The Kurnakov temperature of the bulk β'-CuZn phase is in the range T_k = 741–727 K [16]. It was found that, indeed, in the Zn/Cu film samples deposited onto mica and glass substrates, the SHS reaction between copper and zinc films took place as the temperature T_s was increased to T_0 ($T_s = T_0$). The initiation temperature was in the range 550–600 K, and the SHS front propagation could easily be observed visually (Fig. 1). The initiation temperature T_0 in Zn/Cu/MgO(001) samples was higher by 50–100 K than in the samples deposited on glass substrates, and the SHS front propagation was not distinctly noticeable. The diffraction patterns of the Zn/Cu/MgO(001) samples taken prior to initiation showed that the copper layer grew on the MgO(001) surface epitaxially with the (001) orientation. The absence of reflections from the zinc film deposited on

top of the copper film suggests that it was either finely dispersed or amorphous. As a result of SHS, the copper layer reacted completely since its reflections disappeared. The analysis of diffraction patterns showed that the ordered β' phase and the high-temperature β_2 phase formed in the reaction products (Fig. 2). The ordered β'-CuZn phase is a typical example of the *B*2 phase ordering. The high-temperature β_2 phase probably owes its stability to the higher cooling rate occurring behind the SHS front.

Ni–Zn system. The Ni–Zn system includes only one type *B*2 ordered phase, namely, NiZn. An ordered β_1-NiZn phase of the Cu–Au type is formed as a result of the eutectic-like decomposition at a temperature of T_k = 888 K [16]. The β_1-NiZn phase is stable at room temperature. The Zn/Ni film samples deposited onto the glass substrates, just like the Zn/Cu films (Fig. 1), exhibit a well-defined front when SHS is initiated. The SHS initiation temperature was in the range T_0 = 430–480 K. In Fig. 3, the dependence of the degree of transformation η on the substrate temperature T_s typical of SHS reactions in thin films is shown [10, 11]. The same samples on the MgO(001) substrate had T_0 = 600–650 K. X-ray diffraction by the initial Zn/Ni/MgO(001) samples showed that the nickel film grown on MgO(001) was monocrystalline and contained no zinc reflections (Fig. 4a). The reason for the absence of these reflections is the same as for the Zn/Cu/MnO(001) samples. The measured values of the magnetic crystallographic anisotropy constant of the initial Zn/Ni/MgO(001) samples are close to the value for bulk nickel and confirm that the Ni film grew on MgO(001) epitaxially in the (100) plane. Magnetic and X-ray diffraction measurements showed that SHS in Zn/Ni/MgO(001) samples can penetrate the film thickness only partially. This is possibly caused by intensive heat removal to the substrate and is also observed in Al/Ni/MgO(001) samples [17]. Figures 4b and 4c show diffraction patterns corresponding to the transformation degrees of η = 0.5 and 1, respectively. The new phase must grow epitaxially on the Ni(100) surface since only the strong reflection at d = 0.178 nm is present. However, this reflection does not belong to the ordered β_1-NiZn phase. It has been shown previously [10, 11, 18] that the formation of phases at high SHS front velocities occurs in non-steady-state conditions and the formation of metastable phases and quasi-crystals is possible in the reaction products. Probably, the reflection at d = 0.178 nm belongs either to an unknown metastable phase, a δ-phase, or a $ZnNi_3$ phase with a lattice similar to γ-brass [19]. The large discrepancy between the temperatures T_k = 888 K and T_0 = 430–480 K suggests that the initiation temperature of the first phase in the Zn/Ni film is determined not by the Kurnakov temperature of the β_1-NiZn phase but by an unknown low-temperature structural transformation in the Ni–Zn system.

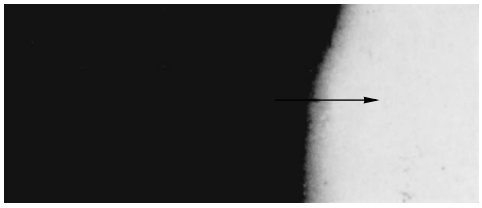

Fig. 1. SHS front in a (150 nm)Zn/(50 nm)Cu film grown on glass substrate. The arrow indicates the front propagation direction.

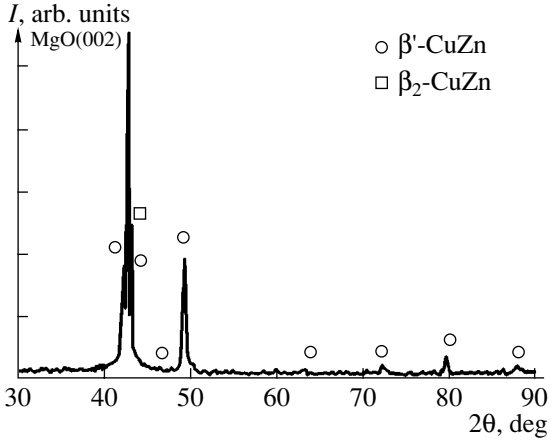

Fig. 2. X-ray diffraction patterns of a (150 nm)Zn/(50 nm)Cu/MgO(001) film sample after passage of the SHS wave.

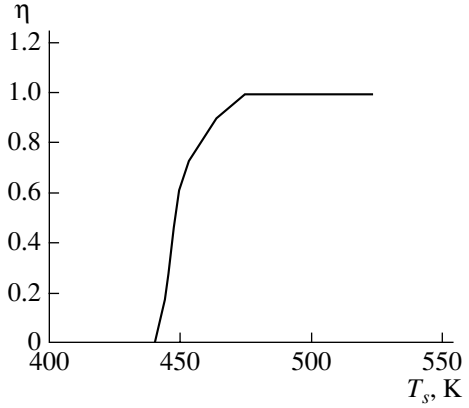

Fig. 3. Degree of transformation η as a function of the substrate temperature T_s in a (150 nm)Zn/(50 nm)Ni bilayer film system.

Ni–Mn system. In the Ni–Mn system, a NiMn phase having $L1_0$ ordering and a Ni_3Mn phase with the $L1_2$ structure are known. The NiMn phase is formed as a low-temperature modification; the Kurnakov temperatures of these phases are T_k(NiMn) = 753 K and $T_k(Ni_3Mn)$ = 778 K, respectively [16]. In the Mn/Ni bilayer samples, propagation of the SHS front could not be seen; therefore, these samples were subjected to RTA. Between the nickel and manganese layers, a

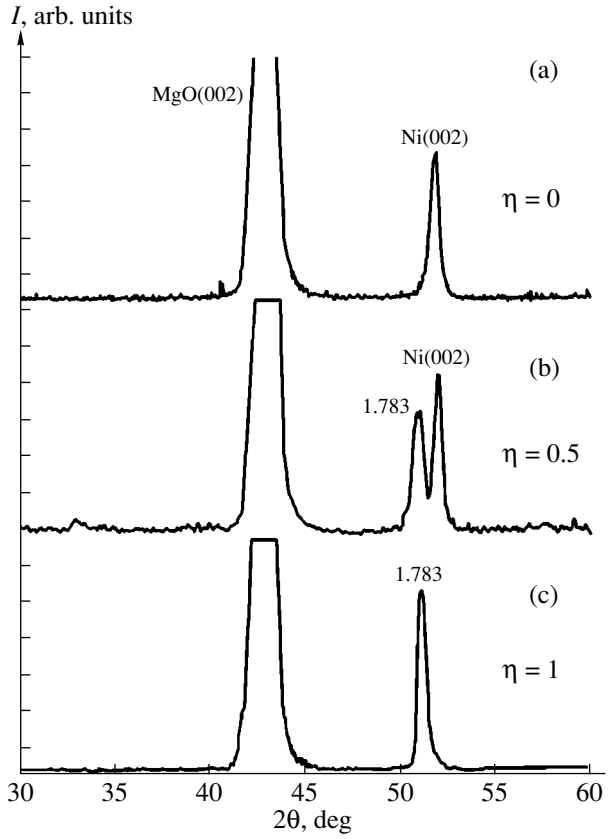

Fig. 4. X-ray diffraction patterns of a (150 nm)Zn/(50 nm)Ni/MgO(001) film sample: (a) initial sample; (b, c) after passage of the SHS front at η = 0.5 and 1, respectively.

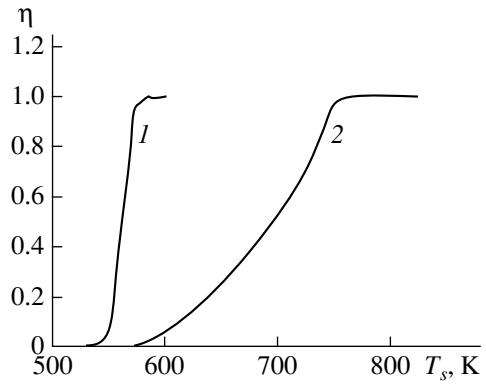

Fig. 5. Degree of transformation η as a function of the substrate temperature T_s in a (100 nm)Mn/(100 nm)Ni bilayer film sample: (*1*) in the course of deposition of the manganese layer onto the nickel layer; (*2*) after rapid thermal annealing.

solid-state reaction took place; in Fig. 5 (curve *1*), the dependence of the degree of transformation η on the substrate temperature is presented for Mn/Ni bilayer samples deposited onto mica substrates. However, it was not expected that $\eta(T_s)$ would depend on the substrate temperature for the Mn layer deposited onto a Ni film (Fig. 5, curve *2*), its initiation temperature (T_0^1 = 570 K) being lower than in the bilayer samples (T_0^2 = 850 K). It has been shown in [10, 11] that during both heating of bilayer samples and consecutive layer deposition from the substrate temperature, the SHS initiation temperature T_0 will be the same. The significant difference between T_0^1 and T_0^2 values suggests different phase formation processes for these two cases of initiation. The Ni–Mn system has been intensively studied mostly on account of the superstructure in Ni_3Mn, which is ferromagnetic in the ordered state. However, no compounds of this system are listed in the JCPDS catalogue. This complicates interpretation of the diffraction patterns of Ni and Mn films successively deposited onto the MgO(100) surface and samples subjected to RTA, which are presented in Figs. 6a and 6b, respectively. The samples containing a reflection for d = 0.178 nm in their diffraction patterns were always ferromagnetic. Therefore, this reflection should correspond to the (002)$MnNi_3$ phase with a lattice constant of a = 0.357 nm [20]. The ordered MnNi phase has a lattice similar to that of CuAu, with a = 0.3714 nm and c = 0.3524 nm [20]. Thus, the reflections for d = 0.221 and 0.185 nm were tentatively assigned to MnNi(111) and MnNi(200) phases. With increase of the RTA temperature, the diffraction patterns change considerably owing to the great diversity of the phase transformations in the Mn–Ni system.

Al–Co system. In the Al–Co system an AlCo alloy with *B*2 ordering is of interest. SHS in thin Al/Co films on glass substrates is initiated at temperatures of 650–680 K. The plots of the degree of transformation as a function of the substrate temperature $\eta(T_s)$ for SHS initiated during deposition and during heating of the Al/Co film samples are identical [10, 11]. The SHS initiation temperature in Al/Co/MgO(001) films is in the range 750–780 K. In Fig. 7, diffraction patterns are presented of the initial Al/Co/MgO(001) samples (Fig. 7a) and after the reaction has taken place (Fig. 7b). The initial samples produced only reflections of the (001)β-Co phase and had no reflection from the aluminum layer deposited on top. As in the film systems discussed above, the top layer was either amorphous or disperse. Analysis of the diffraction patterns and the data on magnetocrystallographic anisotropy of the initial samples showed that the relative orientations of the monocrystalline β-Co film and the substrate were as (001)[100]β-Co ∥ (001)[100]MgO. After passage of the SHS front, which was observed visually, only the AlCo phase was found in the reaction products (Fig. 6b). The presence of the (100) superstructure reflection indicates that the AlCo phase is ordered. Formation of the superstructure in the reaction products suggests that the temperature of the order–disorder transition in the AlCo phase coincides with the SHS initiation temperature in Al/Co bilayer film samples.

Besides the systems considered above, SHS is initiated in bilayer thin samples of Al/Cu (T_0 = 350–400 K), Al/Ti (T_0 = 450–500 K). In respective Al–Cu and Al–Ti systems, CuAl, TiAl, and Ti_3Al superstructures occur [16, 21, 22]. Earlier, it was found [17] that in Al/Fe/MgO(001) films, SHS produces a FeAl superstructure (T_0 = 610–630 K), which, as a film, has an ordering temperature of T_k < 680 K [23]. The closeness of the experimental values of the SHS initiation temperature T_0 in Al/Fe samples and the Kurnakov temperature of the FeAl superstructure suggests that their exact values should coincide. In the Al/Ni/MgO(001) film system, in SHS products, a compound is formed that has been identified as an Al_3Ni_2 phase [17]. This phase is also found after SHS on glass substrates occurring at the initiation temperature (T_0 = 500 K) [10, 11]. Solid-phase reactions in Al/Ni thin films that occur at a temperature T_r ~ 500 K are fairly well studied, with Al_3Ni_2, Al_3Ni, and AlNi phases observed in the reaction products [1, 20, 24, 25]. Equality of the temperatures $T_0 = T_r$ = 500 K testifies that the solid-phase reactions observed in [1, 23–25] proceed in the SHS mode. In the equilibrium state diagram of the Al–Ni system, there is no singularity at a temperature of 500 K. From the foregoing it can be concluded that this temperature might coincide with the ordering temperatures of the phases formed in the reaction products after SHS involving nickel and aluminum layers. It has been shown in [26] that the SHS initiation temperature in Co/Pt, both in bilayers and multilayer films, is close to the Kurnakov temperature of the CoPt bulk alloy [27, 28], which also indicates that these temperatures should be equal in the film state.

Solid-phase reactions were initiated in all thin-film pairs if ordered phases were able to form in the reaction products. However, the initiation temperature of the solid-phase reactions was always lower than the Kurnakov temperature of the alloys formed in the course of the reaction ($T_0 < T_k$). In thin films, the equality $T_0 = T_k$ turns into the inequality $T_0 < T_k$ due to a number of factors: (i) considerable heat removal to the substrate reducing the Kurnakov temperature of thin films in comparison with similar bulk samples; (ii) a high concentration of defects in film condensates; and (iii) the effect on the temperature T_0 of other structural transformations preceding the order–disorder transition and originating in the reaction products.

The foregoing suggests that a one-to-one relation exists between the order in which, with increase of the annealing temperature, the phases form in the bilayer thin films, and the structural transformations in the corresponding binary systems. It appears that the first phase forming at the interface between the films is that which comes first in the phase equilibrium diagram and has the lowest structural phase transitions temperature This rule was first proposed in [26]. Formation of further phases with increase of the annealing temperature

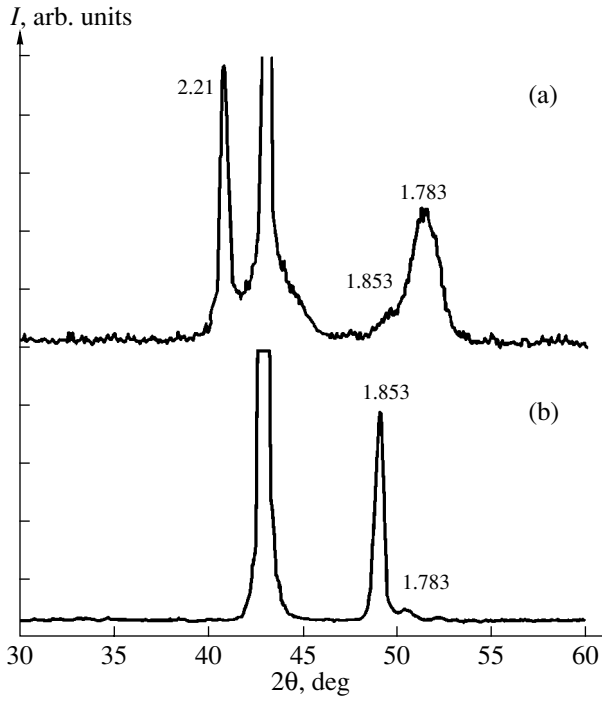

Fig. 6. X-ray diffraction patterns of a (100 nm)Mn/(100 nm)Ni/MgO(001) film sample: (a) after the solid-state reaction during deposition of the manganese layer onto the nickel layer; (b) after rapid thermal annealing cycle.

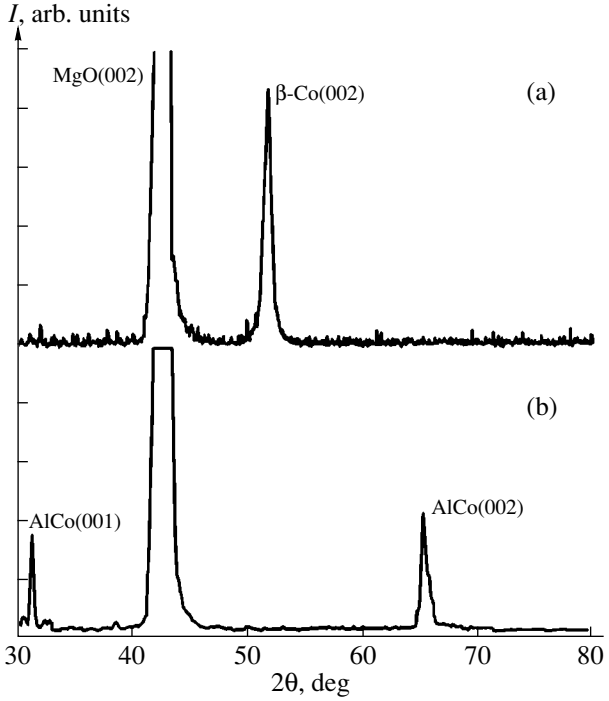

Fig. 7. X-ray diffraction patterns of a (100 nm)Al/(100 nm)Co/MgO(001) film sample: (a) initial sample; (b) after passage of SHS front.

during solid-phase reactions in thin films is governed by structural transitions in a given binary system. The maximum annealing temperature at which the solid-phase reactions occur should coincide with the temperature of the multiple SHS. Therefore, the solid-phase reactions occur in the temperature range found in the phase equilibrium diagram between the eutectic temperature and the minimum temperature of structural phase transformations in a given system. Hence, using the known binary state diagram, the pairs of the component and the initiation temperatures of the solid-phase reactions in the bilayer thin films can be determined. The opposite is possible as well, namely, phase sequences during solid-phase reactions in bilayer thin films can be studied in order to refine the corresponding state diagrams.

It is now widely believed that ordering of atoms into a superstructure occurs via the atoms of the lattice interchanging places. The results of the present work demonstrate that a considerable mass transfer (up to ~200 nm) takes place at the Kurnakov temperature in the film condensates with the formation of alloys. The ordering at $T = T_k$ is only a secondary process. It follows that the long-range mechanism of synthesis determines the ordering processes. The long-range forces can determine the stability of the formed phases and, together with the elastic forces, influence the character of antiphase boundaries in the long-period superstructures, as well as participate in the formation of modulated phases at spinodal and eutectic-like decompositions and in polytype structures.

ACKNOWLEDGMENTS

The work was support in part by the Russian Foundation for Basic Research (project no. 99-03-32184) and the Krasnoyarsk Regional Science Foundation (grant no. 9F12).

REFERENCES

1. *Thin Films: Interdiffusion and Reactions*, Ed. by J. M. Poate, K. Tu, and J. Meier (Wiley, New York, 1978; Mir, Moscow, 1982).
2. E. G. Colgan, C. Cabral, Jr., and D. E. Kotecki, J. Appl. Phys. **77**, 614 (1995).
3. U. A. Clevenger, B. Arcort, W. Ziegler, *et al.*, J. Appl. Phys. **83**, 90 (1998).
4. D. B. Bergstrom, I. Petrov, L. H. Allen, *et al.*, J. Appl. Phys. **78**, 194 (1995).
5. M. Wittmer, P. Oelhafer, and K. N. Tu, Phys. Rev. B **35**, 9073 (1987).
6. W. H. Wang and W. K. Wang, J. Appl. Phys. **76**, 1578 (1994).
7. M. Zhang, W. Yu, W. H. Wang, *et al.*, J. Appl. Phys. **80**, 1422 (1996).
8. T. Nakanishi, M. Takeyama, A. Noya, *et al.*, J. Appl. Phys. **77**, 948 (1995).
9. R. Singh, J. Appl. Phys. **63**, R59 (1988).
10. V. G. Myagkov and L. E. Bykova, Dokl. Akad. Nauk **354**, 777 (1997).
11. V. G. Myagkov, V. S. Zhigalov, L. E. Bykova, *et al.*, Zh. Tekh. Fiz. **68** (10), 58 (1998) [Tech. Phys. **43**, 1189 (1998)].
12. V. G. Myagkov, Dokl. Akad. Nauk **364**, 330 (1999).
13. V. G. Myagkov, L. E. Bykova, and G. N. Bondarenko, Zh. Éksp. Teor. Fiz. **115**, 1756 (1999) [JETP **88**, 963 (1999)].
14. V. G. Myagkov, L. E. Bykova, V. S. Zhigalov, *et al.*, Dokl. Akad. Nauk **371**, 763 (2000) [Dokl. Phys. **45**, 157 (2000)].
15. V. G. Myagkov, L. E. Bykova, G. N. Bondarenko, *et al.*, Pis'ma Zh. Éksp. Teor. Fiz. **71**, 268 (2000) [JETP Lett. **71**, 183 (2000)].
16. N. M. Matveeva and É. V. Kozlov, *Ordered Phase in Metallic Systems* (Nauka, Moscow, 1989).
17. V. G. Myagkov, L. E. Bykova, and G. N. Bondarenko, Dokl. Akad. Nauk **368**, 615 (1999) [Dokl. Phys. **44**, 667 (1999)].
18. V. G. Myagkov, L. E. Bykova, and G. N. Bondarenko, Pis'ma Zh. Éksp. Teor. Fiz. **68**, 121 (1998) [JETP Lett. **68**, 131 (1998)].
19. N. I. Ganina, A. M. Zakharova, V. G. Oleĭnicheva, *et al.*, in *Constitution Diagrams of Metallic Systems* (VINITI, Moscow, 1988), Vol. XXXII.
20. M. Hansen and K. Anderko, *Constitution of Binary Alloys* (McGraw-Hill, New York, 1958; Metallurgizdat, Moscow, 1962), Vol. 2.
21. T. Muto and J. Tacagi, *The Theory of Order-Disorder Transitions in Alloys*, in *Solid State Physics: Advances in Research and Applications*, Ed. by F. Seitz and C. D. Turnbull (Academic, New York, 1955; Inostrannaya Literatura, Moscow, 1959).
22. C. S. Barrett and T. B. Massalski, *Structure of Metals: Crystallographic Methods, Principles and Data* (Pergamon, Oxford, 1980; Metallurgiya, Moscow, 1984), Part 1.
23. V. Y. Kudryavtsev, V. V. Nemoshkalenko, Y. P. Lee, *et al.*, J. Appl. Phys. **82**, 5043 (1997).
24. E. Ma, C. V. Thompson, L. A. Clevenger, *et al.*, Appl. Phys. Lett. **57**, 1262 (1990).
25. J. C. Liu, J. W. Mayer, and J. C. Barbour, J. Appl. Phys. **64**, 656 (1988).
26. C. Michaelsen, G. Lucadamo, and K. Barmak, J. Appl. Phys. **80**, 6689 (1996).
27. V. G. Myagkov, L. A. Li, L. E. Bykova, *et al.*, Fiz. Tverd. Tela (St. Petersburg) **42**, 937 (2000) [Phys. Solid State **42**, 968 (2000)].
28. K. Barmak, R. A. Ristau, K. R. Coffey, *et al.*, J. Appl. Phys. **79**, 5330 (1996).

Translated by M. Lebedev